EPJ Web of Conferences **71**, 00026 (2014)
DOI: 10.1051/epjconf/20147100026

Study of the $\mu^+ \to e^+\gamma$ decay with the MEG experiment at PSI: present and future

Paolo Walter Cattaneo[1,a]

[1] *INFN Pavia, Via Bassi 6, 27100, Italy*

Abstract. The results of the data collected by the MEG detector at the Paul Scherrer Institut during the three years of operation (2009-2011) in search for the lepton flavor violating decay $\mu^+ \to e^+\gamma$ are presented. The design and expected performances of the MEG upgrade to be operated in the coming years are sketched.

1 Introduction

Charged lepton flavor transitions are forbidden in the minimal Standard Model because of the vanishing neutrino masses. The introduction of neutrino masses and mixing induces flavor transitions radiatively, but at a negligible level. In fact the expected branching ratio for $\mu \to e\gamma$ is $\sim 10^{-50}$. The observation of charged lepton flavor transitions would represent a clear signal of physics beyond the Standard Model being virtually background free. In the following the MEG experiment, devoted to the search of the $\mu^+ \to e^+\gamma$ decay, is described; its results, based on the 2009-2011 data sample, are shown and the prospects of an upgrade are presented.

2 The physics case of the MEG experiment

Chearge lepton flavor transitions with branching ratios at a level reachable by experiments are suggested by many theories extending the Standard Model [2–4]. The main transitions involving Charge Lepton Flavor Violation (CLFV) are (l indicates e or μ):

$$\mu \to e\gamma \quad \mu \to eee \quad \mu N \to eN$$
$$\tau \to e\gamma \quad \tau \to \mu\gamma \quad \tau \to lll$$

The comparison between $\mu \to e\gamma$ versus $\mu \to eN$ conversion and $\mu \to eee$ is usually done in a model independent way by using the effective Lagrangian [1]

$$\mathcal{L}_{CLFV} = \frac{m_\mu}{(\kappa+1)\Lambda^2}\bar{\mu}_R\sigma_{\mu\nu}e_L F^{\mu\nu} + \frac{\kappa}{(\kappa+1)\Lambda^2}\bar{\mu}_R\gamma_\mu e_L \bar{f}\gamma^\mu f \tag{1}$$

which contains two terms contributing to CLFV. In the second one f stands for the appropriate fermion field: the electron in the $\mu \to eee$ case or the relevant quarks in the $\mu \to eN$ conversion case. While

[a] e-mail: Paolo.Cattaneo@pv.infn.it

Table 1. Relative sensitivities and experimental limits of the main CLFV processes.

Process	Relative probability	Present Limit	Experiment	Year
$\mu \to e\gamma$	1	5.7×10^{-13}	MEG	2012 [7]
$\mu^- Ti \to e^- Ti$	$Z\alpha/\pi$	4.3×10^{-12}	SINDRUM II	1993 [12]
$\mu^- Au \to e^- Au$	$Z\alpha/\pi$	7.0×10^{-13}	SINDRUM II	2006 [13]
$\mu \to eee$	α/π	7.0×10^{-12}	SINDRUM	1988 [11]
$\tau \to e\gamma$	$(m_\tau/m_\mu)^{2-4}$	3.3×10^{-8}	Belle/BBar	2011 [14]
$\tau \to \mu\gamma$	$(m_\tau/m_\mu)^{2-4}$	4.4×10^{-8}	Belle/BBar	2011 [14]

$\mu \to e\gamma$ proceeds only via the first term, corresponding to $\kappa = 0$, the $\mu N \to eN$ conversion process and the $\mu \to eee$ decay may proceed also through the other one (large κ values). Figure 2 shows the range of parameters in the (κ , Λ) plane that can be explored by $\mu \to eN$ conversion, $\mu \to eee$ or $\mu \to e\gamma$ experiments.
All the relevant SUSY - GUT models privilege the $\kappa = 0$ term for which one can see from Fig. 2 that MEG is not only competitive with the second phase of the $\mu \to eee$ experiment but also with the first phase of the Mu2e project.
In this region approximate scaling laws for the various CLFV decays are reported in Table 1

3 The MEG experiment

The MEG experiment is designed to search for $\mu \to e\gamma$ with a sensitivity of $O(10^{-13})$. The signature of $\mu \to e\gamma$ is a pair of monochromatic (52.8 MeV) positron and photon emitted with 180° opening angle, at the same time. The dominant background is the accidental coincidence of a high momentum Michel positron and a high energy photon from a radiative muon decay or annihilation-in flight (AIF) of a Michel positron. Another type of background is the radiative muon decay with the emission of very low energy neutrinos. To achieve high sensitivity, a high rate muon beam and a detector with high resolution and efficiency are necessary. In order to reduce the accidental background rate, it is important to reduce the material around the muon stopping target, which can produce AIF photons when hit by positrons from muon decays. The accidental background rate is proportional to the square of the muon decay rate; a continuous muon beam is therefore preferrable for $\mu \to e\gamma$ search experiments.
The MEG experiment is located at the E5 area of the Paul Scherrer Institut (PSI), exploiting a continuous muon beam with intensity $3 \times 10^7 \mu^+$/s provided by a 1.3 MW proton cyclotron.

Figure 2 shows the MEG detector [7]. The muon beam is stopped in the muon stopping target, which is a 205 μm thick polyethylene sheet. The target is slanted at 20.5° to optimize the stopping efficiency of muons, the multiple scattering of signal positrons and the background photon rate from AIF. The stopping efficiency is 82%.
For the physics-event trigger, the FPGA based system requests the photon energy to be higher than a threshold (45 MeV), the time-coincidence between a photon and a positron and the direction match of the two particles. The DAQ rate is about 10 Hz. Signals from the detector is digitized by Domino Ring Sampler (DRS) [16] chips, that contain a switched capacitor array with 1024 cells, and input waveforms are digitized with a sampling frequency of 0.8 and 1.6 GHz depending on the subdetector. Positron detectors are located inside a COnstant Bending RAdius (COBRA) superconducting solenoid, which provides a special gradient magnetic field. The field strength is maximum (1.27 T) at the center and becomes weaker at the edge (0.49 T). Because of the special configuration of the field, positrons are quickly swept out; thus the hit rate of the Drift CHambers (DCH) is reduced.

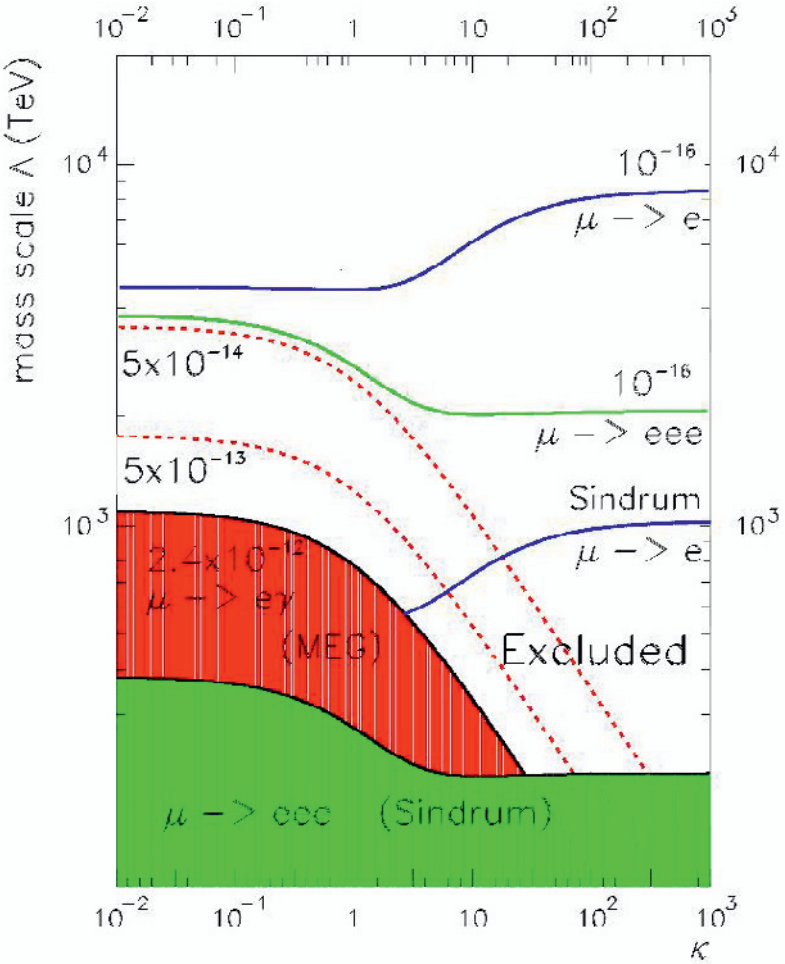

Figure 1. The range of parameters in the (Λ , κ) plane that are explored by $\mu \rightarrow e\gamma$, $\mu \rightarrow eee$ and $\mu \rightarrow eN$ conversion experiments (adapted from [10]).

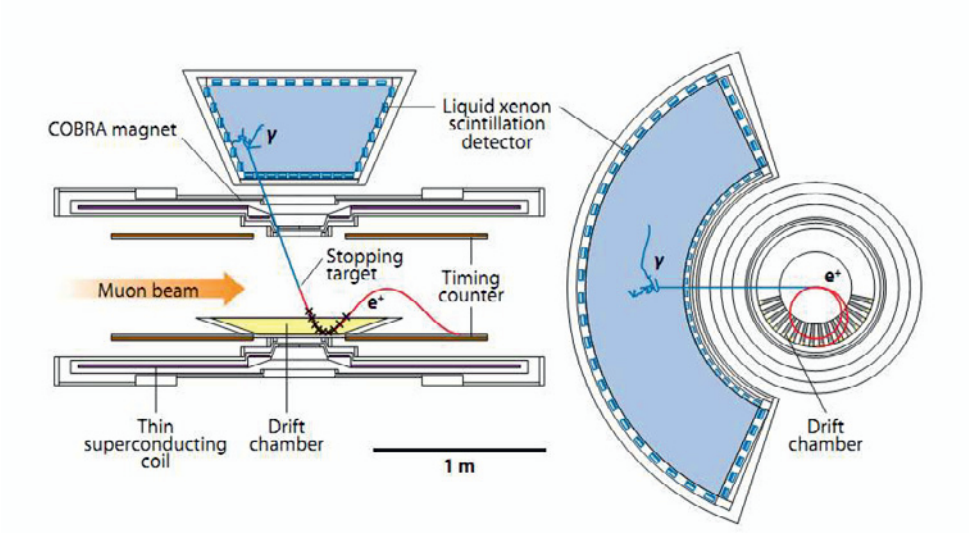

Figure 2. The MEG detector.

The bending radius of the positron trajectories is weakly dependent on the polar angle, which allows to place the DCH only in the large radius region to detect high-momentum positrons (> 40 MeV) efficiently without increasing the hit-rate due to low-momentum positrons too much.
The DCH system consists of 16 radially aligned modules. In order to reduce the multiple scattering and the AIF photons, there is no frame structure at the inner part. The system is built with light materials; the amount of material traversed by a positron in one turn in average corresponds to 2×10^{-3} X_0.
The momentum resolution is measured from the measured spectrum of Michel positrons. The vertex position resolutions and the positron angle resolutions are measured by using events where two turns of a positron are measured by DCH.
The time of positrons is measured by the Timing Counters (TC), which consists of long thick plastic scintillation counters, operated in a magnetic field, read out by fine-mesh PhotoMultiplier Tubes (PMT). The time resolution of the TC is measured to be 65 ps by comparing the measured hit-time of Michel positrons on adjacent TC bars.
The Liquid Xenon (LXe) scintillation calorimeter detects photons reaching it traversing the COBRA magnet. In 900 liters of liquid xenon, 846 PMTs are placed to detect scintillation photons.
For the calibration, several kinds of gamma ray sources, from 4.4 MeV to 129 MeV, are used. The resolution and efficiency are measured by using 54.9 MeV photons from the decays of π_0 produced by Charge EXchabge reactions (CEX). To take CEX data, the muon beam is switched to a pion beam once or twice per year.
The relative time resolution between a photon and a positron from a muon decay is measured by using radiative muon decay events. The resolutions and efficiencies are summarized in Table 2.

Table 2. Resolutions (Gaussian sigma) and efficiencies for MEG and the upgraded MEG. The positron vertex resolutions refer to horizontal and vertical directions. The photon position resolutions refere to horizontal, vertical and depth directions. The photon energy resolutions refer to shallow conversion events (<2 cm) and deeper (> 2 cm). For the positron vertex position and energy resolutions, the σs of the core components are shown.

Resolutions	Present	Upgrade
e^+ energy (keV)	306	130
e^+ θ (mrad)	9.4	5.3
e^+ ϕ (mrad)	8.7	3.7
e^+ vertex (mm)	2.4/1.2	1.6 / 0.7
γ energy (%)	2.4/1.7	1.1/1.0
γ position (mm)	5.0/5.0/6.0	2.6/2.2/5.0
γ-e^+ timing (ps)	122	84
Efficiencies		
trigger	$\approx$ 99	$\approx$ 99
γ	63	69
e^+	40	88

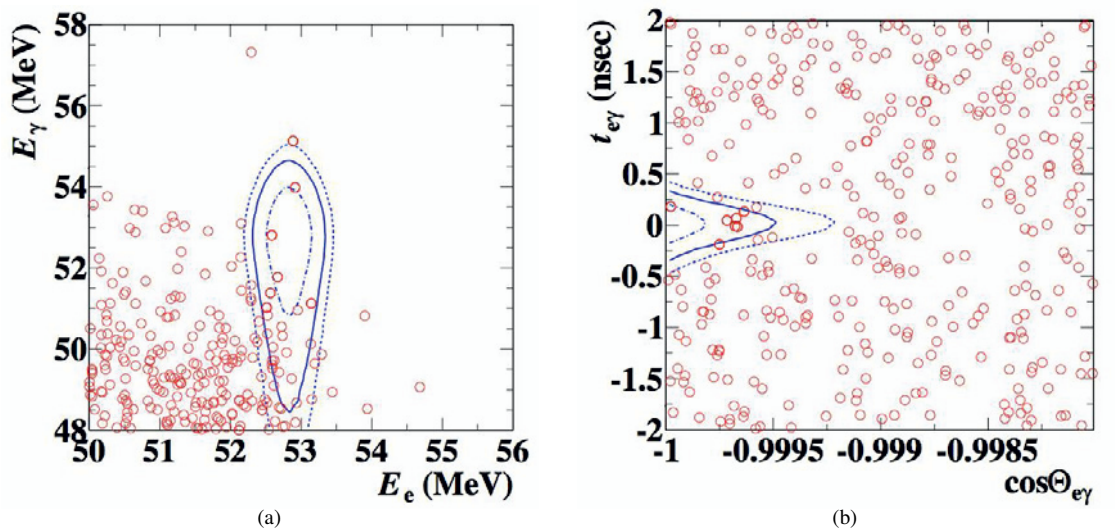

(a) (b)

Figure 3. Events in the 2009–2011 dataset around the analysis region. In the right plot, $\Theta_{e\gamma}$ is the stereo angle between the photon and the positron. The three contours in each plot show the regions covering the signal PDF 39.3, 74.2 and 86.5%, respectively. Event selections ($|t_{e\gamma}| < 244.3$ ps and $\cos\Theta_{e\gamma} < 0.99963$) and ($51.0 < E < 55.5$ MeV and $52.385 < Ee < 55.0$ MeV) are applied for the left and for the right plots, respectively.

4 Latest results

We analyzed data taken in years 2009–2011. At the start of the 2011 data taking, the buffering scheme of the trigger and the readout system were changed from the single-buffer to the multiple-buffer one. Thanks to the change, the DAQ livetime became about 99% and the signal efficiency became 97%.
The precision of the position measurements of the DCH modules and the muon stopping target was improved by using a new optical alignment system. The data quality of the LXe detector calibration was improved by replacing NaI detectors, which is used to measure the opening angle of two photons from a π_0 decay, with BGO detectors. In the waveform analysis of DCH, an FFT based offline noise reduction was added. By noise reduction, the signal efficiency is improved by 6% and the angular resolutions are improved by a few %. The track fitting algorithm for positrons was revised. In the new algorithm, a more detailed description of the detector geometry and a better hit-model are used. Thanks to the new algorithm, the signal efficiency is improved by 7% and the tail component of the detector response is reduced.
A new method of pile-up unfolding of multiple photons entering the LXe detector was developed. The new method can unfold pile-up photons with 7% higher signal efficiency than the previous one. The tail component of the energy response is reduced.
The likelihood analysis is used to extract the best fit and the confidence interval of the number of signals (Nsig) in datasets. The distributions of five observables, photon energy (E_γ), positron energy (E_e), time difference between a photon and a positron ($t_{e\gamma}$) and two opening angles between the two particles ($\theta_{e\gamma}$ and $\phi_{e\gamma}$), are fitted by a function which is the sum of three functions corresponding to the signal, the muon radiative decay and the accidental background. The amplitude of the three functions are free parameters in the fitting. Most of the probability density functions (PDF) are extracted from the calibration or physics data. The PDFs for the radiative muon decay is formed from the theoretical spectrum and the detector responses. The confidence interval is calculated by using a frequentist method with a profile likelihood-ratio ordering. The numbers of background events are treated as nuisance parameters. The systematic uncertainties are included in the confidence intervals by randomizing PDF parameters according to their uncertainties. For the data taken in 2011, we used the blind analysis technique; namely events around the signal region, selected by using E_γ and $t_{e\gamma}$, are not used for the calibrations and the optimization of analysis parameters. The normalization factor to convert Nsig to the branching ratio is calculated by counting the number of positrons from Michel decays during the physics data taking. The difference of efficiency for the signals and for the Michel positrons is taken into account. The normalization factor for the 2009–2011 dataset is 7.77×10^{12}.
The expected upper limit at 90% confidence level is calculated as the median of the upper limits of an ensemble of pseudoexperiments. The sensitivity of the analysis of 2009–2011 dataset is 7.7×10^{-13}.
The likelihood analysis is done on the time-sideband data to check the level of backgrounds in data. No excesses of the signal were found, and the upper limits are 1.6×10^{-12} and 8.1×10^{-13} for the negative and positive time-sidebands, respectively.
Figure 3 show the events around the analysis region. In the analysis region, no excess of events is found. The upper limit of the branching ratio is calculated to be 5.7×10^{-13} at 90% confidence level. This limit is the most stringent to date, and constrains strongly new physics models.
The expected sensitivity for the full MEG dataset until 2013 is 5×10^{-13}.

5 The MEG2 upgrade

The MEG collaboration plans to search for $\mu \to e\gamma$ with one order of magnitude better sensitivity. A proposal of the upgrade of the experiment was approved by PSI [9]. To achieve the goal, a higher beam intensity, a higher detection efficiency and better detector resolutions are needed.

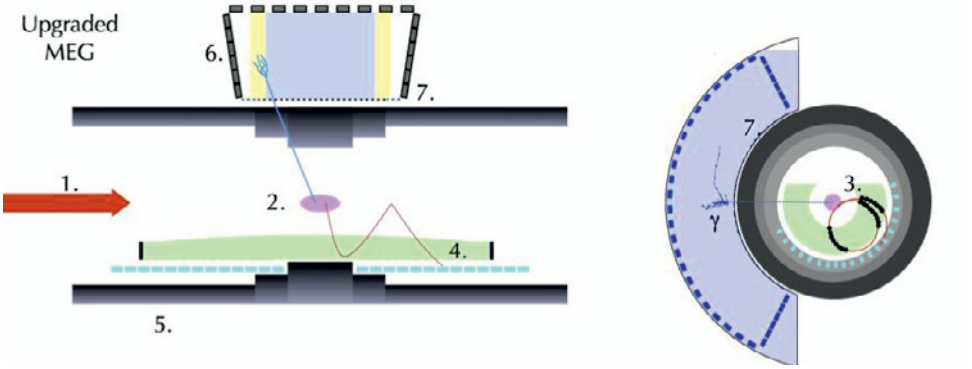

Figure 4. The upgraded MEG detector: 1: muon beam, 2: muon stopping target, 3: drift chamber(s), 4: timing counters, 5: solenoid, 6: liquid xenon photon detector.

More than twice higher muon beam rate than the present MEG is already possible in the E5 area. In order to suppress the multiple-scattering of positrons and AIF photons generated in the target, in the baseline design, a thinner (140 m) target is foreseen for the upgraded MEG. The slant angle of the target is decreased to 15° to stop the muons efficiently. The muon stopping rate is estimated to be 7×10^7 μ/s. Figure 4 shows the present and the upgraded detectors. The new DCH has a long unique gas volume. The new TC will consist of many small plastic scintillation plates; the scintillation photons are detected by SiPMs attached at the both ends. The photon sensors on the inner face of the LXe detector will be replaced by SiPMs.

In the present spectrometer, about half of signal positrons can hit the frame or the amplifier boards of DCH before entering TC. For a higher transparency for positrons going through DCH toward TC, the new DCH has a long gas volume, so that most of the signal positrons can travel to TC without being hardly scattered. The detection efficiency for the signal positrons is expected to be $> 85\%$.

The average amount of material in one turn of the positron trajectories is 1.7×10^{-3} X_0, smaller than that of the present DCH. The stereo angle wire configuration was chosen for the reconstruction of the longitudinal coordinate. The larger number of hits in the large gas volume compared to the present DCH will improve the momentum and angular resolutions. Currently several prototypes are under test.

For the new TC, small scintillation plates, whose size is $\sim 90 \times 40 \times 5$ mm, are being considered. The average number of counters hit by a signal positron is ~ 6. By averaging the multiple hit-times, the overall time resolution for signal positrons will be 35 ps including the contributions from the multiple-scattering and from the time-jitter of electronics. Beam tests will be conducted to check that the multiple-hit scheme achieves the expected resolution.

The inner face PMTs in the LXe detector will be replaced by SiPMs. That makes the light collection efficiency more uniform over the position of light sources. The width of the inner face will be increased and the direction of lateral PMTs will be changed for a better energy resolution for photons entering near the lateral faces. The total effect on the energy response and position resolutions are estimated by using simulations. Because SiPMs are much thinner than PMTs, the amount of material in the inner face will be decreased, which makes the detection efficiency higher by 10%.

To cope with the increased number of readout channels, the trigger and readout electronics will be also upgraded. In the present experiment, the waveform digitizers for triggering and for those used in the physics analysis are separated. The trigger system reads the waveforms continuously with a

low sampling frequency; upon request, DRS boards read waveforms with high frequencies. For the upgraded MEG, a new digitization board (WaveDREAM) is being developed. In the WaveDREAM boards, the trigger and the high frequency readouts are integrated on the same board. Wave-DREAM Table 2 summarizes the improvements of the detector performance.
In three years of data taking, the expected data statistics, taking into account the higher beam rate, the higher detector efficiency and a more efficient use of the beam time compared to the present MEG will be one order of magnitude higher than the full statistics of MEG.
The expected sensitivity is calculated by using the same analysis framework with the present MEG. The expected upper limit on the branching ratio assuming the null hypothesis is 5×10^{-14}.

6 Conclusion

The MEG experiment has searched for the CLFV decay $\mu \to e\gamma$ with data collected in 2009-2011. The sensitivity of the analysis is 7.7×10^{-13}. No excess of the signal was found, and the upper limit on the branching ratio is 5.7×10^{-13} at 90% confidence level. MEG has collected data until 2013, doubling the statistics. The final sensitivity is expected to be $5. \times 10^{-13}$.
A proposal for upgrading MEG is presented including a new unique-volume cylindrical drift chamber, a new timing counter consisting of scintillator plates and an upgraded LXe detector with SiPMs on the inner face, The upgraded MEG is planed to start in year 2016; the expected sensitivity is 5×10^{-14} with three years of data taking.

References

[1] A. de Gouvea and N. Saoulidou, Annu. Rev. Nucl. Part. Sci., **80** 513 (2010)
[2] Barbieri, R. and Hall, L. , Phys. Lett. B **338**, 212 (1994)
[3] Barbieri, R. and Hall, L. and Strumia, A., Nucl. Phys. B **445**, 219 (1995)
[4] Hisano J et al., Phys. Lett. B **391** 341 (1997)
[5] Marciano W J, Mori T. and Roney J. M., Annu. Rev. Nucl. Part. Sci. **58** 315 (2008)
[6] Adam J. et al, Phys. Rev. Lett. **107**, 171801, (2011)
[7] Adam J. et al., Eur. Phys. J. C **73** 2365 (2013)
[8] Adam J. et al, Phys. Rev. Lett. **110**, 201801, (2013)
[9] Baldini A. M. et al, "MEG Upgrade Proposal", ArXiv:1301:7225 [physics.ins-det]
[10] R.M. Carey and others, FERMILAB PROPOSAL 0973: http://mu2e.fnal.gov
[11] Bellgardt, G. et al., Nucl. Phys. B **299**, 1 (1988)
[12] Dohmen, C. et al., Phys. Lett. B **317**, 431 (1993)
[13] Bertl, W. et al., Eur. Phys. J. C **47**, 337 (2006)
[14] Aubert B. et al., Phys. Rev. Lett. **104**, 021802 (2010)
[15] Aubert B. et al., Phys. Rev. Lett. **104**, 021802 (2010)
[16] Ritt S. et al, Nucl. Instr. and Meth. A **623**, 486 (2010)